International Solar Energy Society

Conference Proceedings

EuroSun 2014
Aix-les-Bains (France), 16 - 19 September 2014

Experimental and numerical studies of a porous material for a new indirect regenerative cooling system

Guilian Leroux[1,2], Louis Stephan[2], Nolwenn Le Pierrès[1], Etienne Wurtz[2]

1 LOCIE, Université de Savoie, CNRS UMR5271, Le Bourget du Lac (France)

[2] SBST, CEA, Le Bourget du lac (France)

Abstract

This paper presents the experimental and numerical results of evaporative tests through a porous material to be used in a novel evaporative cooling system for low-energy buildings.

The critical component of the cooling system is a porous tank used as a heat exchanger and evaporator. The temperature of the water contained in the tank decreases because of radiation, convection and evaporation at the tank surfaces. The cooled water is then used to meet the cooling demand of a building, using a water to air heat exchanger.

The aim of this paper is to choose a porous material and to determine experimentally its characteristics, particularly the water flux through the material the material, and the mass transfer coefficients. These data will then be used to calibrate the numerical model of the tank and predict the cooling potential of the proposed system.

1. Introduction

Energy used for buildings needs represents as much as 40% of world's total energy use. Heating, ventilation and air conditioning (HVAC) account for 50% of a building's energy consumption (Perez-Lombard and al, 2007). In emerging countries with hot climates such as India, air conditioning is planned to grow rapidly (Chaturvedi and al, 2014). In France, the air conditioning equipment rate in buildings increases regularly: in 2007 it reached 4% for residential buildings and 20% for tertiary buildings. This rate is quite low in comparison with the United States and Japan, but it continues to increase. Traditional compression refrigeration systems involve on high electricity consumption; moreover, fluorocarbons commonly used as refrigerants are known to be responsible for ozone depletion. It is urgent to develop innovative low-energy consumption systems to handle this increasing air conditioning demand. In this context, evaporative cooling systems may be valuable solutions.

2. Review on evaporative cooling technologies

Evaporative cooling is an ancient technique based on the phase change of water. Latent heat needed for water evaporation is significant. During evaporation, energy is taken from the surroundings and thus decreases its temperature. This potential can then be used for cooling purpose, like buildings air conditioning.

This technique has long been used passively in Africa and the Middle East. Evaporative systems such as roof ponds or interior terra cotta tanks are still in use but their potential is limited. During the last few years, active evaporative cooling systems have received considerable attention, and numerous studies have been

Selection and/or peer review under responsibility of EuroSun2014 Scientific Committee
doi:10.18086/eurosun.2014.11.01 Available at http://proceedings.ises.org

conducted on this topic. The simplest system is the direct evaporation cooling system (DEC); water is directly sprayed into a ventilation air flow, decreasing its temperature before blowing it inside the building. This system is simple but its drawback is that brings water into the building and may result in moisture issues. This problem is solved with the indirect evaporative cooling system (IEC). In this system, there are two different air flows. In the first one, water is sprayed, its temperature decreases, it passes through an air/air heat exchanger before being rejected outside. The second air flow cools passing through the heat exchanger and is channeled inside the building. Among the numerous studies on this subject is a review of the different IEC designs (Duan and al, 2012), and another article (Joudi, 2000), which experimentally compares direct and indirect evaporation systems. These systems are limited in wet climate areas where the air is often saturated because the evaporation potential is low. To solve this problem, a desiccant material can be used to dry the airflow before using it in an evaporative cooling process. Desiccant material can be liquid or solid; the most well-known application is the desiccant wheel. Experimental and numeric studies (Bourdoukan, 2008, Maalouf 2006) have been conducted on this system; although it shows good results, it remains complicated and expensive.

Cooling systems taking advantage of sky radiation and convection with the air during the night are also available. Radiant panels are set on a roof, with water running through pipes in these panels. The water temperature decreases and the water is then be used for cooling purposes. Heidarinejad and al (2010) describes this type of system coupled with a DEC system.

Cooling systems taking advantage of both the sky radiation and evaporative cooling have appeared over the last few years. This kind of system is set up on the ZAE Bayern in Wurtzburg (Büttner, 2014) and on the Carnegie Institution of Washington Global Ecology Center roof located in Stanford, CA. Water runs on the roof during the night; evaporation, convection and radiation decrease the water temperature. The cool water is then stocked and used during the day. Other systems use a porous tank. Water from the tank reaches the outside surface passing through the porous layer, and evaporation occurs at the surface and cools the tank and its contents. Experimental studies show a temperature difference up to 8°C between the water in the tank and the outside temperature (Ibrahim and al, 2003, He and Hoyano, 2010).

3. The cooling system

Evaporative cooling is already a widespread technology. The system described in this paper is based on the analysis of existing systems. The system described herein aims to use three heat transfer modes simultaneously (radiation, evaporation and convection) to reach very low maintenance effort, low cost and high efficiency. The important components of the system illustrated in Figure 1 are the storage tank (1), the porous tank made with terra cotta (3), a heat exchanger (2), a pump (5) and a control valve (7).

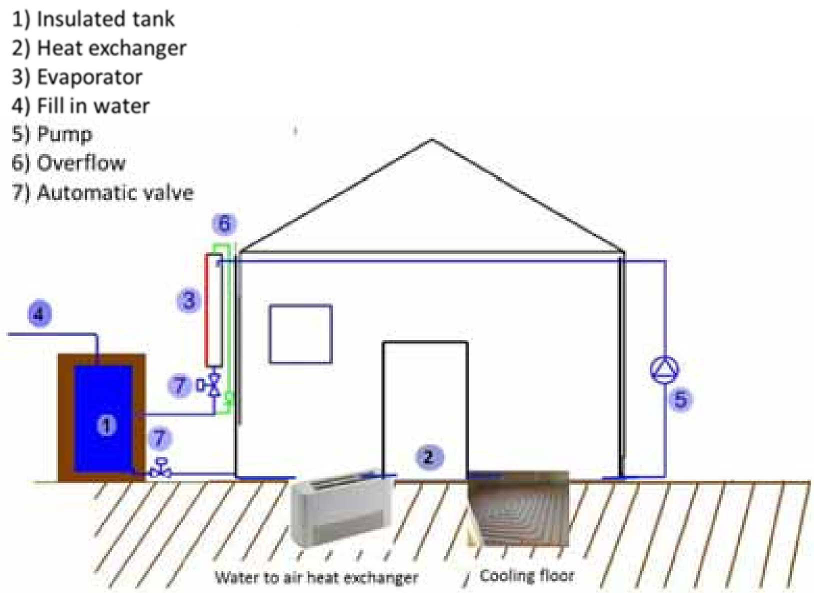

Fig. 1: Working plan of the cooling system integrated into a dwelling

The system follows a daily cycle. In the morning, as soon as the temperature of the water contained in the porous tank (3) begins to increase, the control valve opens and cool water flows into the storage tank (1). During the day, when the inside house temperature exceeds the comfort temperature, cool water passes through the heat exchanger (2), removes heat from the building and then is stocked in the porous tank (3). During the following night, evaporation, convection and radiation cool water in the porous tank and the cycle can begin again.

4. Experimental study of the porous material

The key component of the system is the porous tank. An experimental study is conducted to find the best material to use for this application. We have focused on terracotta because it is a very inexpensive and strong material, and its raw material (clay) is widespread and available in very large amounts. Moreover, the previous studies on cooling systems using porous material used terra cotta (Ibrahim and al, 2003).

4.1. Experimental setting

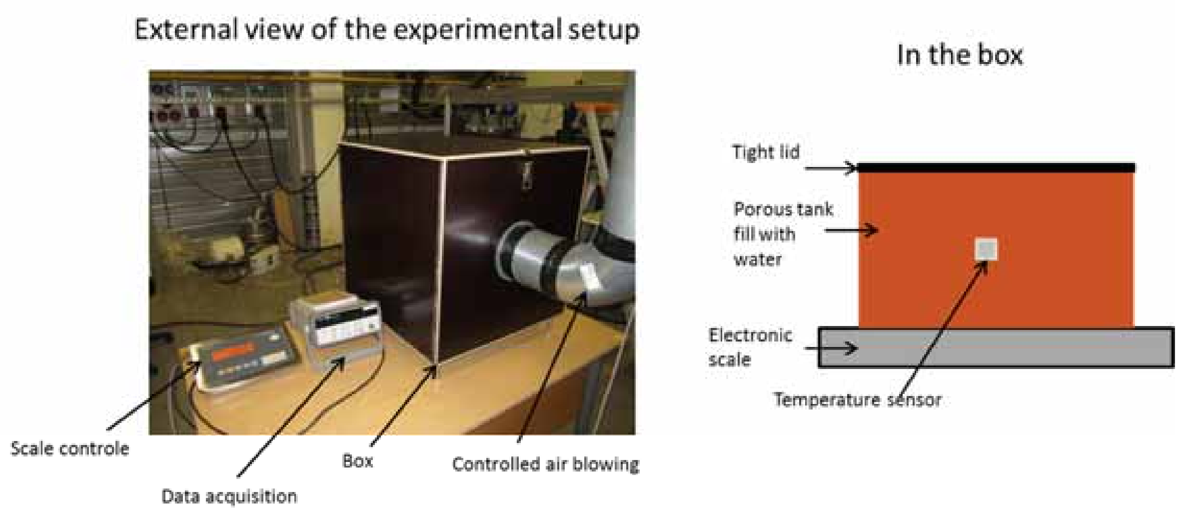

Fig. 3: Experimental setup

The experimental setting (Figure 2) is composed of an air conditioning unit, preparing an air flow with the desired temperature, humidity and flow rate. Uncertainty is ±6% on the flow rate, ±0.6 g_w/kg_{dryair} on humidity and ±0.5 K on temperature. The porous tank is set in a 0.6 m×0.6 m×.06-m cube, connected to the airflow with a 16 cm diameter flow duct. The box is drilled at its back for the air flow to go out so that the box is crossed by a controlled air flow.

4.2. Measurements

The porous tank is set on a Sartorius scale with 0.2g precision; this scale records changes in mass and thus the evaporation rate. Temperature sensors are set in the water, on the outside surface of the tank and at the entrance of the air flow. The sensors are calibrated with a 0.2-K measurement precision.

4.3. Terra cotta comparison

Five different terracottas were tested, common products found in DIY stores: a brick (by Wienerburger) and four flowerpots numbered from 1 to 4. The brick and pot 4 are rectangular; their sizes are reported in Table 1 with H the height, L the length and p the depth. Pots 1–3 are truncated cones with h the height, d_1 the largest diameter and d_2 the smallest diameter, e is the thickness of walls.

First, the porosity of the terra cotta was measured. The porosity of a material P is the ratio between the pores' volume and the total volume; it can be calculated with formula (1) knowing the wet mass m_w, the dry mass m_d and the immersed mass of the sample i.e., the mass of the sample plunged into the liquid (water).

$$P = \frac{V_{pore}}{V_{total}} = \frac{m_w - m_d}{m_w - m_{im}} \quad \text{(eq. 1)}$$

A hydrostatic scale was used to measure this immersed mass. Secondly, the water evaporation rate is measured with the experimental setting described above. The characteristics of the air flow are velocity, 2.8 m/s; temperature, 27.6°C and absolute humidity, 13.5g of water per kg of dry air, equivalent to a 60% relative humidity. The main results are reported in Table 1.

Tab. 1: Results of evaporation tests on terra cotta comparison

	T_a(°C)	T_w(°C)	ΔT(°C)	ΔP(Pa)	dm	Size	Porosity
Brick	28.1	24.7	3.4	910.0	2.01	$H = 0.25, L = 0.3, p = 0.1, e = 0.007$	33.6%
Pot 1	27.6	25.1	2.5	1010.0	3.25	$h = 0.2, d_1 = 0.2, d_2 = 0.14, e = 0.007$	25.2%
Pot 2	27.5	23.3	4.2	691.0	3.60	$h = 0.155, d_1 = 0.175, d_2 = 0.10, e = 0.013$	31.2%
Pot 3	27.7	26.2	1.5	1220.0	0.85	$h = 0.13, d_1 = 0.14, d_2 = 0.09, e = 0.006$	17.0%
Pot 4	27.7	27.0	0.7	1310.0	0.35	$H = 0.11, L = 0.32, p = 0.10, e = 0.014$	23.0%

In this table, T_w is the water temperature in the porous tank, T_{air} is the blowing air temperature, ΔT is the temperature difference between air and water, ΔP is the difference between the vapor pressure at the tank surface (the tank surface is considered to be saturated) and the partial pressure of water in the air flow $\Delta P = P_{vsat}(T_{surf}) - P(T_{air})$. dm (g/min/m²) is the evaporation rate per surface of material, HR is the relative humidity. P_{vsat} is calculated from the Clapeyron formula (eq (2)).

$$p_{sat}(T) = p_0 e^{\frac{M.L_v}{R}\left(\frac{1}{T_0} - \frac{1}{T}\right)} \qquad p_v(T) = HR.p_{sat}(T) \quad \text{(eq. 2)}$$

In these formulas, M=18 g/mol is the molar mass of water, Lv=2257 kJ/kg is the water's latent heat of evaporation, R=8.31 J/mol/K is the ideal gas constant, T_0=373.15 K the temperature and P_0 the pressure at the reference state.

The results show important differences between tested pots, for exemple evaporation rate of pot 2 is more than ten times higher than for pot 4. We can observe that the highest evaporation rates are obtained with the most porous pot. This pot also gives the largest difference in temperature between water and blowing air. Moreover, the rectangular shape shows poor results because a large proportion of the surface is not exposed to the airflow since it arrives perpendicular to the tank.

This comparison shows that different materials can lead to big differences in evaporation rate and water temperature and emphasizes how important, the choice of the material for the evaporative system is. The cylindrical pot (n°4) with high porosity gives the best results; a comprehensive study on this pot was thus undertaken.

4.4 Study on pot number 2

Figure 3 (a) shows the pot studied with its main geometric features. The first experiment was undertaken with no air flow, relative humidity of 30%. Figure 3(b) shows the temperature change during the experiment. When the steady state is reached, air temperature is 19.9°C, and the water temperature is 15.6°C. The evaporation rate is 1.22 g/min/m².

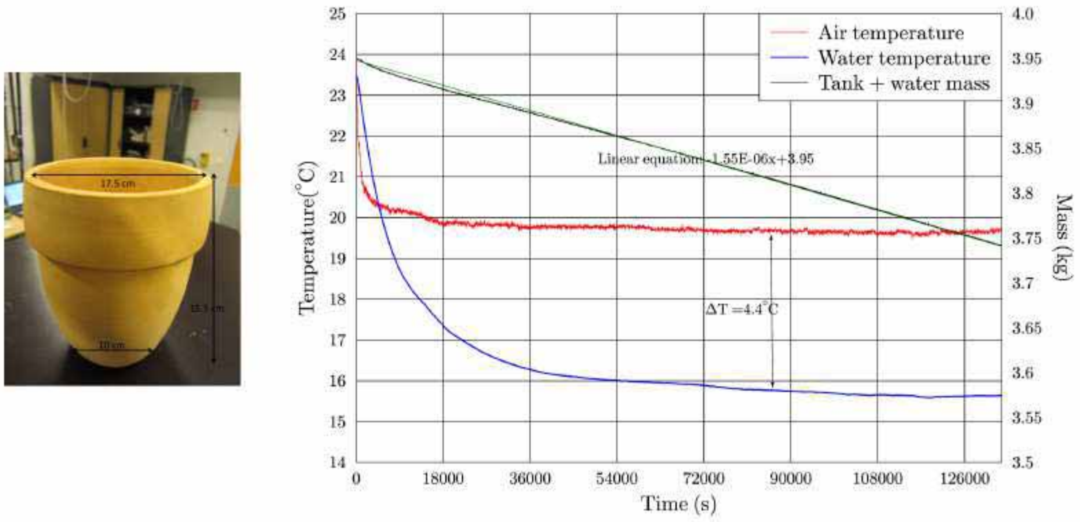

(a) (b)

Fig. 3: Pot number 2 (a); outside air temperature, water tank temperature and changes in mass during a case with no air flow

A series of tests was performed on the pot, varying the air flow rate and the humidity of the blowing air. Table 2 and Figure 4 report the main results. In Table 2, the evaporation rate, mass transfer coefficient and temperature difference changes with the water pressure difference ΔP and the air velocity in the box are given, with H_a, the absolute humidity of the blowing air (g_{wat}/kg_{dryair}).

Table 2: Evaporative tests results on pot n°4

	H_a	T_{air}(°C)	T_{water}(°C)	ΔT(°C)	ΔP(Pa)	$\dot{m}$ (g/min/m^2)	h(s/m)
1m/s	2	25.8	19.5	6.3	1935	2.84	2.4e-08
	5	25.8	19.9	5.9	1518	2.47	2.7e-08
	10	25.9	21.4	4.5	939	2.06	3.7e-08
	13.5	25.9	22.2	3.7	514	1.57	5.1e-08
2.8m/s	2	27.5	21.5	6.0	2220	4.74	3.6e-08
	5	27.5	22.2	5.3	1880	4.31	3.8e-08
	8	27.4	22.8	4.6	1450	4.14	4.8e-08
	10	27.5	23.2	4.3	1240	3.73	5.0e-08
	13.5	27.4	24.0	3.4	848	3.03	5.9e-08
5.5m/s	2	28.3	23.9	4.4	2597	5.44	3.5e-08
	5	28.3	24.2	4.1	2119	4.90	3.9e-08
	8	28.4	24.7	3.7	1769	4.56	4.3e-08
	10	28.4	25.0	3.4	1518	4.41	4.8e-08
	13.5	28.3	25.3	3.0	1020	3.81	6.2e-08

Figure 4 shows that the evaporation rate increases with the air velocity and the water vapour pressure difference. However, the increase in the evaporation rate is slightly low between the air velocity of 2.8 m/s and 5.5 m/s, which might indicate that the amount of water going through the terra cotta from the tank to the outside is insufficient to keep the outside surface of the tank wet. The mass transfer coefficient increases with air velocity and decreases with water pressure difference.

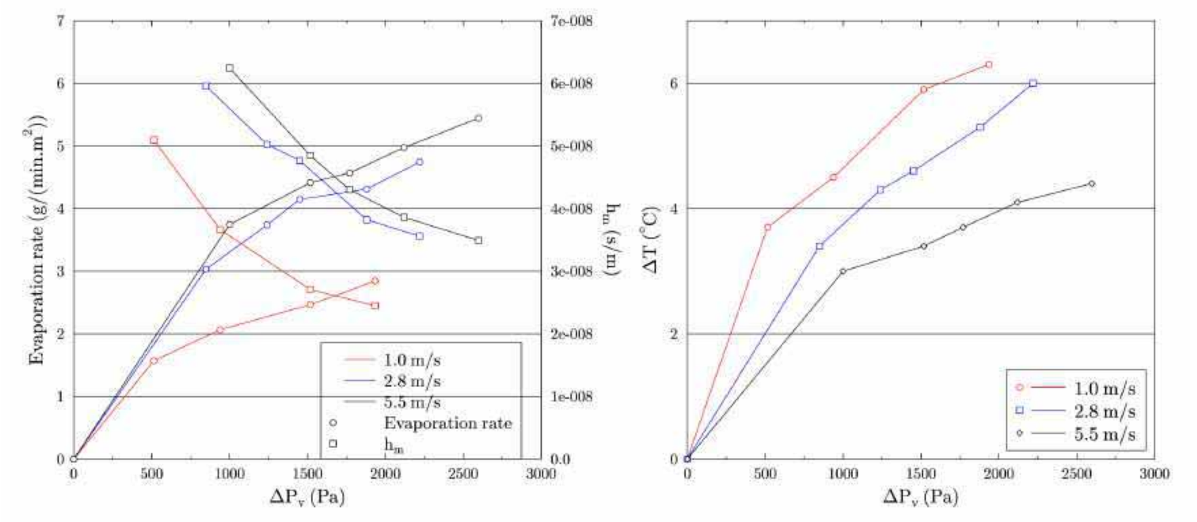

Fig. 4: Changes in evaporation rate, mass transfer coefficient (left) and temperature difference between air and water (right) as a function of blowing air velocity and water pressure difference.

We can see that the temperature difference between water and blowing air decreases with the air velocity and increases with the water pressure difference. At steady state, there is a balance between evaporation, which removes heat from the tank, and convection, which gives heat to the tank. With low air velocities convection is low and temperature differences are high; in contrast, with high air flow the convective heat is high and the evaporation heat doesn't increase enough to compensate the convection that lead to a small ΔT. In our experimental setup, there is a competition between evaporation and convection, but for future real use, during the night, the water temperature inside the porous tank should be greater than the outside air temperature. Convection and evaporation effects will be added to cool the water until the water temperature reaches the air temperature, and then competition between these transfers modes will start.

5. Modeling of the porous tank

The purpose of this section is to develop, test and calibrate a nodal model representing the thermal behavior of the porous tank. This model will be compared to experimental results and used for more general applications. It is developed with Modelica Dymola.

5.1. Convection ϕ_{conv} (W)

The pot is considered as a cylinder set perpendicular to the air flow. The Churchill and Bernstein correlation (Churchill and Bernstein, 1977) is used to calculate the convective heat transfer coefficient.

$$\overline{Nu}_D = 0.3 + \frac{0.62 \mathrm{Re}_d^{1/2} \mathrm{Pr}^{1/3}}{\left[1 + (0.4/\mathrm{Pr})^{2/3}\right]^{1/4}} \left[1 + \left(\frac{\mathrm{Re}_d}{282000}\right)^{5/8}\right]^{4/5} \quad \overline{Nu}_D = \frac{\overline{h}_D \lambda}{D} \qquad \text{(eq. 3)}$$

With Nu the Nusselt number at the cylinder surface, Re_d the air flow Reynolds number, Pr the Prandtl number, h_D the convective heat transfer coefficient at the cylinder outside surface (W/m²/K), d and D, the duct diameter and cylinder diameter, and λ the thermal conductivity of air (W/m/K).

Convective heat ϕ_{conv} (W) is then:

$$\Phi_{conv} = A.\overline{h}_D(T_{surf} - T_{ext}) \qquad \text{(eq. 4)}$$

with A the tank area (m²) and T_{surf} its temperature (°C).

5.2. Radiation ϕ_{rad} (W)

Radiant heat is calculated with (eq 5):

$$\Phi_{rad} = A\sigma\epsilon(T_{surf}^4 - T_{rad}^4) \qquad T_{rad}^4 = f_v T_{sky}^4 + (1 - f_v)T_{ext}^4 \quad \text{(eq. 5)}$$

with f_v the view factor of the porous tank to the sky, σ the Boltzmann constant, ε the surface emissivity and T_{sky} the sky temperature calculated from the Martin correlation (Martin and Berdahl, 1984).

5.3. Evaporation ϕ_{evap} (W)

Evaporation heat is proportional to the evaporation rate, latent heat L and evaporation surface A.

$$\Phi_{evap} = AL_v\dot{m}$$

$$\dot{m} = h_m(P_{sat}(T_{surf}) - P_v(T_{air})) \quad \text{(eq. 6)}$$

For the mass heat transfer coefficient h_m, we use experimental results described in the preceding section.

5.4. Conduction

The thermal conductivity of the porous material saturated with water is considered equal to 0.77 W/(m.K). The internal heat resistance between the water and the porous tank wall is not taken into consideration.

5.5. Water saturation

To keep wet the outside surface of the porous tank, the evaporation rate should be lower than the water flow rate through the material. The water flow rate depends on the porous organization of the terra cotta. We consider that the material is always wet and saturated. However, this hypothesis is no longer valid for high air velocities and will be improved in future models.

6. Modeling and comparison with experimentation

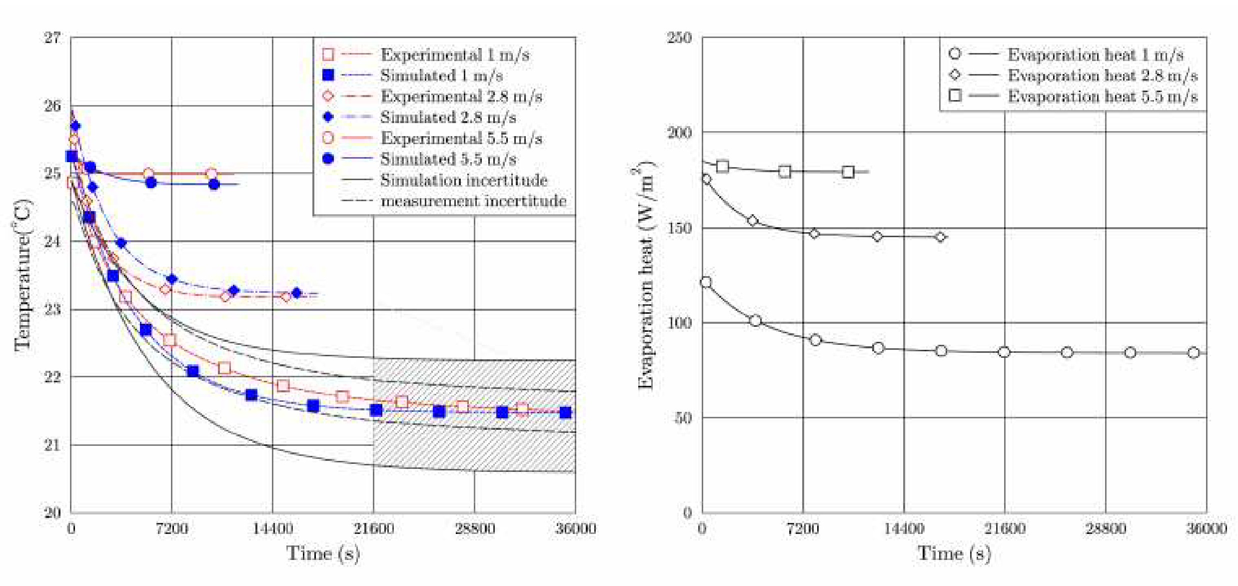

Fig. 5: Measurement/ modeling comparison (left) and simulated evaporation heat (right)

The model and experimental results on the changes in water temperature in the porous tank are compared in different conditions with constant air velocity, outside temperature and humidity. Three comparisons are made and illustrated in Figure 5 with an absolute humidity of 10 g/kg, blowing air speed of 1, 2.8 and 5.5m/s. The blowing air temperature is 26, 27.5 and 28.5°C. At steady state, the temperature difference between experiment and simulation is low (less than 0.2°C), but in the dynamic period at the beginning we can observe up to 0.5°C difference. Evaporative heat ranges from 75 to 200 W/m^2: the higher the air velocity, the more powerful the system is. The modeling uncertainty for temperature is around 1°C at steady state. The shading zones in Figure 5 show this uncertainty. The experimental temperature is inside the uncertainty area. Dynamic comparisons will further be analysed to improve and validate the model.

7. Conclusion

This paper reports works on porous materials that can be used in an innovative cooling system based on water evaporation. Different terracottas have been compared and results show that for evaporative cooling applications, terracotta with high porosity is suitable. More experimental investigations have been lead on the pot giving the best results. Evaporation process at the outside surface of this pot can cool water down to 4.4°C below the outside air temperature without wind with a relative humidity of 30%. Experiments with different air velocity have been conducted and show temperatures difference between the water temperature inside the tank and the outside air temperature up to 6°C.
Preliminary results are compared with a simple model. This model shows good agreement with experiments and will be used to size the system in order to test it on an actual house.
These results offer promising futur to this innovative cooling system and emphasize the importance of the choice of the porous material.

8. References

Bourdoukan, P., 2008. Étude numérique et expérimentale destinée à l'exploitation des techniques de rafraîchissement par dessiccation avec régénération par énergie solaire. PhD thesis, Laboratoire Optimisation Conception et Ingénieurie de l'Environnement.

Büttner, D. D. 2014. Regenerative cooling system.

Chaturvedi, V., Eom, J., Clarke, L.E., Shukla, P.R., 2014. Long term building energy demand for India: Disaggregating end use energy services in an integrated assessment modeling framework. Energy Policy. 64, 226-242.

Churchill, S.W., Bernstein, M,. 1977. A correlating equation for forced convection from gases and liquidsto a circular cylinder in cross_ow. J. Heat Transfer, 99 :300_306.

Duan, Z., Zhan, C., Zhang, X., Mustafa, M., Zhao, X., Alimohammadisagvand, B., Hasan, A., 2012. Indirect evaporative cooling: Past, present and future potentials. Renewable and sustainable Energy Reviews. 16, 6823-6850.

He, J., Hoyano, A., 2010. Experimental study of cooling e_ects of a passive evaporative cooling wall constructed of porous ceramics with high water soaking-up ability. Buildings and environment. 45 :461_472.

Heidarinejad , G., Farahani, M.F., Delfani, S., 2010. Investigation of a hybrid system of nocturnal radiative cooling and direct evaporative cooling. Building and Environemnt. 45 :1521_1528.

Ibrahim, E., Shao, L., Riffat, S.B., 2003. Performance of porous ceramic evaporators for building cooling application. Energy and buildings. 35 :941_949.

Joudi, K.., 2000. Application of indirect evaporative cooling to variable domestic cooling load. Energy conversion and management. 45: 461:472.

Maalouf, C., 2006. Étude du potentiel de rafraîchissement d'un système évaporatif à désorption avec régénération solaire. PhD thesis, Laboratoire Optimisation Conception et Ingénieurie de l'Environnement.

Martin, M. and Berdahl, P., 1984. Characteris tics of infrared sky radiation in the united states. Solar Energy, 33 :321_326.

Perez-Lombard, L., Ortiz, J., Pout, C., 2007. A review on buildings energy consumption information. Energy and buildings. 40, 394-398.